

Reprinted from

Symposium on

Machine Processing of

Remotely Sensed Data

June 27 - 29, 1979

The Laboratory for Applications of
Remote Sensing

Purdue University
West Lafayette
Indiana 47907 USA

IEEE Catalog No.
79CH1430-8 MPRSD

Copyright © 1979 IEEE
The Institute of Electrical and Electronics Engineers, Inc.

Copyright © 2004 IEEE. This material is provided with permission of the IEEE. Such permission of the IEEE does not in any way imply IEEE endorsement of any of the products or services of the Purdue Research Foundation/University. Internal or personal use of this material is permitted. However, permission to reprint/republish this material for advertising or promotional purposes or for creating new collective works for resale or redistribution must be obtained from the IEEE by writing to pubs-permissions@ieee.org.

By choosing to view this document, you agree to all provisions of the copyright laws protecting it.

COMPUTER RECOGNITION OF CITRUS INFESTATIONS

D.H. WILLIAMS

The University of Texas at El Paso

J.K. AGGARWAL

The University of Texas at Austin

ABSTRACT

A computer software system is described that uses digitized color information from aerial color infrared transparencies to detect the presence of citrus mealybug (*Pseudococcus citri* Risso), brown soft scale (*Coccus hesperidum* L.), and Rio Grande gummosis in individual citrus trees. The color coordinates at each spatial point, and color differences at adjacent points are used to locate the trees and to detect the infestations; and compensation is made for the variation in color characteristics between different transparencies. The system requires the input of four parameters: a flag denoting the presence of heavy shadows in the image, nominal tree size and spacing of the citrus trees, and a flag denoting the season of the year when the transparency was taken. An index of recognition, I_q , was defined and used as a measure of recognition effectiveness. For unknown data, I_q ranged from 43% to 81%, with nominal values of 60% to 80% for all three infestations.

I. INTRODUCTION

Each year in the United States, citrus mealybug, brown soft scale and Rio Grande gummosis cause serious economic losses to citrus growers in the form of damaged trees, lower yields, and depreciated fruit. Presently, this damage is assessed by formal or informal ground surveys, or by human interpretation of aerial color infrared (CIR) transparencies. Previous investigations¹⁻⁷ have found that many citrus infestations exhibit identifiable features in low altitude CIR images. Unfortunately, some of the infestations are not readily distinguishable from each other, however. Other work^{8,9} has determined that machine recognition of citrus infestations is feasible, using an interactive processing system with an operator assisting in the decision-making process. The present study extends this work with the development of a software system that operates in a batch environment, recognizing the infestations

The research was supported in part by the National Science Foundation under grant ENG74-04-986.

using only four parameters as input. Brown soft scale, citrus mealybug, and Rio Grande gummosis were chosen for this processing since they tend to exhibit unique characteristics on CIR film, and because they cause damage in all of the growing areas of the United States. (Rio Grande gummosis is known by other names¹⁰ in growing areas outside of Texas.)

In color infrared transparencies, the infestations^{1-3,11} are characterized primarily by changes in the light reflected from the leaves. Healthy tree foliage exhibits a bright red appearance due to strong reflectance of near infrared wavelengths. In contrast brown soft scale and citrus mealybug excrete a honeydew solution which provides an excellent growth site for the sooty mold fungus *Capnodium citri* Berk. and Desm. The presence of the mold is sensed by the film, since the reflectance from the foliage is greatly reduced in both the visible and near infrared spectral regions, giving a dark red or black appearance. The two infestations can be distinguished by the distribution of the mold: brown soft scale is characterized by a heavy coating of mold that appears black or dark red while mealybug causes an uneven coating that exhibits a mottled black and red appearance.

Gummosis is a disease that is caused by unknown agents that attack the main branches or upper trunk of the tree. Nutritional deficiencies cause leaves in the affected area to turn chlorotic (yellow-green) in color, increasing the reflectance in the visible light region. This increase is manifested in CIR film as a white or pink color.

The input data for the system consists of color transparencies that are digitized using a color¹² flying spot scanner, and transformed into a normalized^{8,13} color coordinate system. At each spatial point, the normalized coordinate values are:

$$I = (R+G+B)/3 \quad (1)$$

$$X = 255 \cdot R / (R+G+B) \quad (2)$$

$$Y = 255 \cdot G / (R+G+B) \quad (3)$$

where

R, G and B are the red, green, and blue color intensities output by the scanner.

I is the intensity (brightness) coordinate value.

$$0 \leq I \leq 255$$

X and Y are the red and green chromaticity coordinates respectively; $0 \leq X \leq 255$ and $0 \leq Y \leq 255$, where X and Y are set to zero if $I = 0$.

The response for each spatial point is described by a three dimensional space, with two coordinates representing chromaticity, and the

third intensity.

II. DATA CHARACTERISTICS

In order to determine the general characteristics of the data, selected areas of the eight training slides identified in Table 1. were scanned to obtain their distributions in the (X,Y,I) space. The mean values of these distributions, normalized to a range of 0 to 1, are shown in Figure 1. Analysis¹⁴ of this information determined that three classes of data could be defined and modeled in the (X,Y) plane as shown in Figure 2, since for each of the three infestations, coordinate values of the infested foliage clustered between those from background features, and from healthy tree foliage. Furthermore, since the slope of the class axis varied by only a small amount between different slides, a new chromaticity coordinate, W, was defined as a linear combination of X and Y:

$$W = 301X - 203Y + 54 \quad (4)$$

This transformation simultaneously reduces the dimensionality of the data while maximizing the between class separation of the three classes. The effect of this transformation is shown in Figure 3, where the mean values from Figure 1 are replotted in the (W,I) domain.

SLIDE NUMBER	IDENTIFICATION	
1	G-5	G = gummosis
2	G-1	
3	BSS-5	BSS = brown soft scale
4	BSS-6	
5	BSS-12	
6	MB-4	MB = mealybug
7	MB-7	
8	MB-2	

Table 1 Training Slide Identification

Further processing determined that the training slides exhibited large variations in chromaticity and intensity characteristics in the (W,I) space due to differences in film exposure, ambient light conditions, and scanner gain levels during processing. However, by normalizing the coordinate values with respect to the maximum and minimum values of W and I, the coordinates for healthy and infested tree foliage clustered in four regions as shown in Figure 4. (As will be described shortly, these regions are used to determine the tree classification parameters.)

III. PROCESSING

The processing for detection and classification of the three infestations uses both spectral (color) and spatial information from the

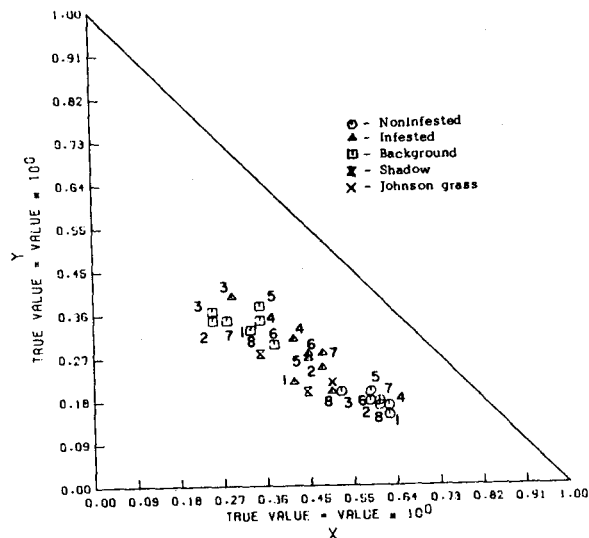


Figure 1 (a) Mean Values of the Training Slide Color Distributions in the X,Y Plane

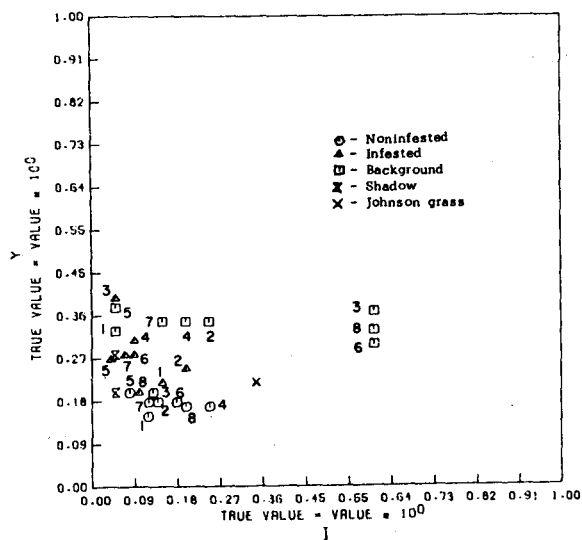


Figure 1 (b) Mean Values of the Training Slide Color Distributions in the I,Y Plane

image. Selective processing of the data is employed to reduce the amount of computation. The processing consists of three parts: location of individual citrus trees within rectangular boundaries, preprocessing to compensate for the variation in color characteristics between different slides and to determine the parameters needed for classification, and classification of

the health of each tree.

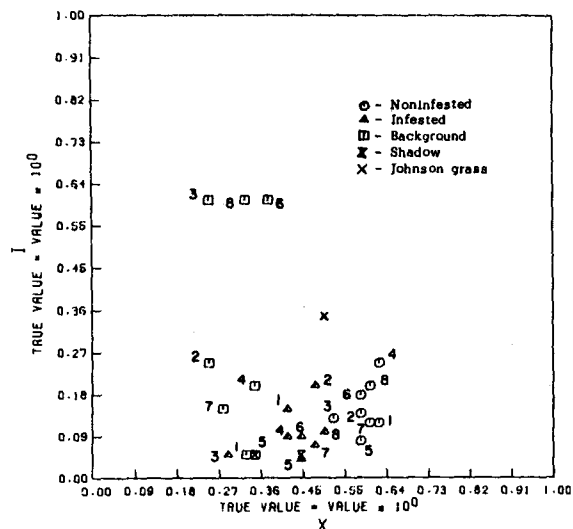


Figure 1 (c) Mean Values of the Training Slide Color Distributions in the X,I Plane

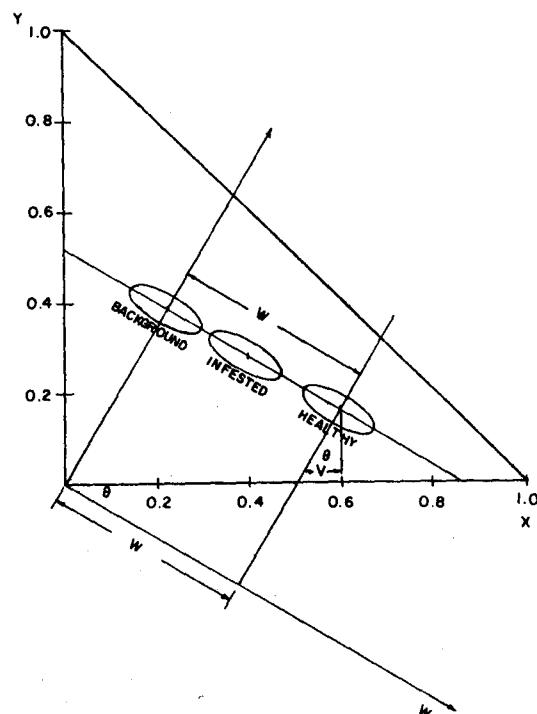


Figure 2 Coordinate Transformation

Tree location requires the input of two parameters: the nominal tree size and tree

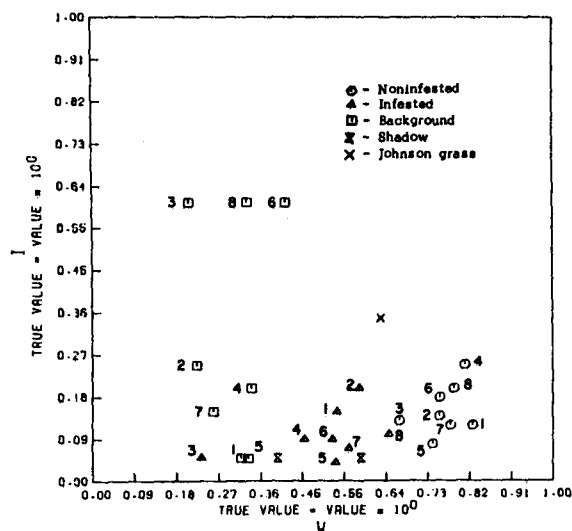


Figure 3 Mean Values of the Training Slide Color Distributions in the W,I Plane

spacing; and restrictions on the input images that the citrus trees be planted in a regular pattern, that the individual trees not be completely grown together, and that the transparencies be taken at an altitude of 10,000 feet or less. Only the W coordinate is used in this step, since the background and tree foliage coordinates are separated primarily along the W axis as shown in Figure 3.

The image is scanned in vertical strips as shown in Figure 5, using a directional derivative 15, 16 that is averaged across the width (one nominal tree size and one nominal tree spacing) of each strip to locate vertical edges:

$$DIF = \sum_{K=K1}^{K2} (W(J,K) - W(J-1,K)) \quad (5)$$

where

DIF is the averaged directional derivative for row J of a given strip

K1, K2 are the column bounds for that strip

W(J,K) is the W coordinate value for location (J,K)

As the directional derivative is calculated down a strip, leading and trailing edges of treelike objects exhibit positive and negative peaks. If successive positive and negative peaks exceed preset thresholds, the vertical separation is calculated to determine whether it is within a

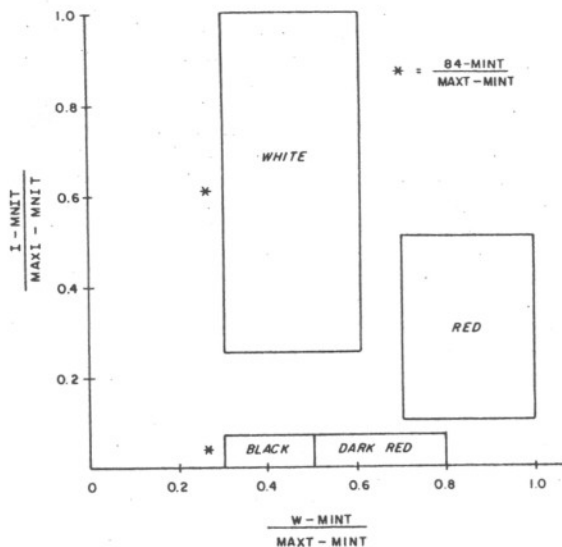


Figure 4 Color Search Regions

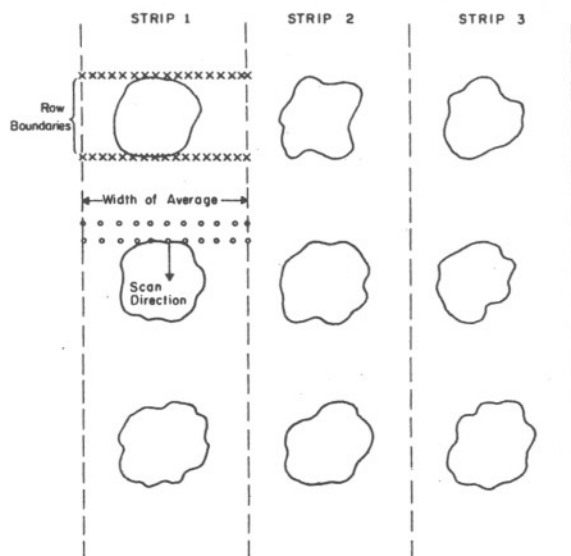


Figure 5 Vertical Scan

size window of 7/10 to 10/7 of a nominal tree size. If the size is acceptable, the edge coordinates are stored as vertical tree boundaries; otherwise, the scanning proceeds as before.

After all of the vertical strips have been scanned, the image is next scanned horizontally between the vertical boundaries, using the same process as previously. As before, if the thresholding and size criteria are satisfied, the left and right edge coordinates are stored with the top and bottom values.

Upon completion of the horizontal scan, ECN, a measure of the difference in vertical and horizontal size is calculated for each object in which the boundaries have been stored in the previous steps:

$$ECN = (TOP - BOT) / (RSIDE - LSIDE) \quad (6)$$

where

TOP is the top boundary

BOT is the bottom boundary

RSIDE is the right boundary

LSIDE is the left boundary

If the following inequality is satisfied:

$$0.6 < ECN < 1.66 \quad (7)$$

the vertical and horizontal size of the object are of the same order and the object is assumed to be a tree; otherwise, the four boundaries of the object are erased.

A citrus grove infested with mealybug is shown in Figure 6, and a plot of the averaged directional derivative for a vertical scan strip of this image is shown in Figure 7. Each tree row causes a positive peak at the top edge of a tree row that falls off rapidly, forming a negative peak at the bottom edge. Consequently, seven sets of positive and negative peaks are exhibited, one for each row of trees. The rectangular boundaries for the trees are shown in Figure 8.

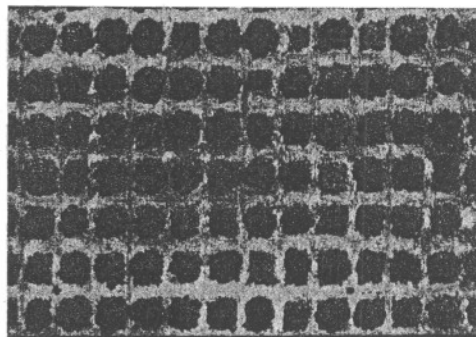


Figure 6 Slide MB-2

To preprocess the data, the spatial points within the tree boundaries are scanned in two passes. During the first pass, the maximum and minimum values of the W and I coordinates are determined. MAXT and MINT, and MAXI and MINT are the maximum and minimum values for W and I respectively, as shown in Figure 4. To compensate for the variation in color characteristics, the coordinates at each spatial point can be normalized, or the fixed boundaries in the normalized

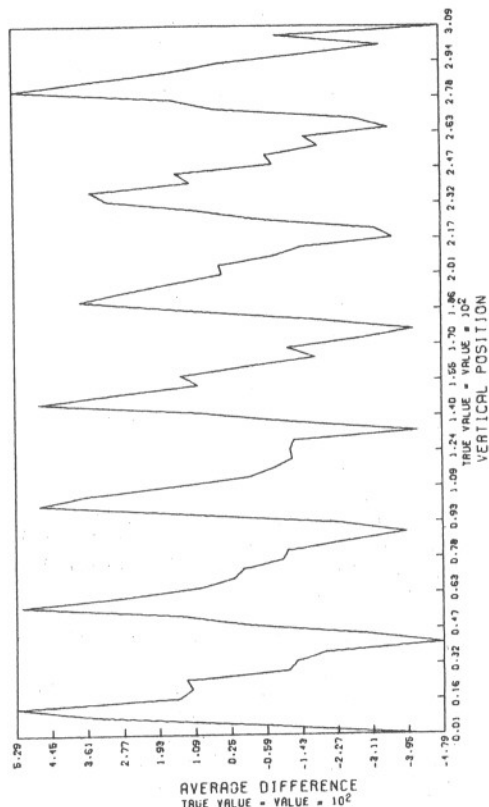


Figure 7 Fourth Vertical Scan Strip
K = 133 - 173

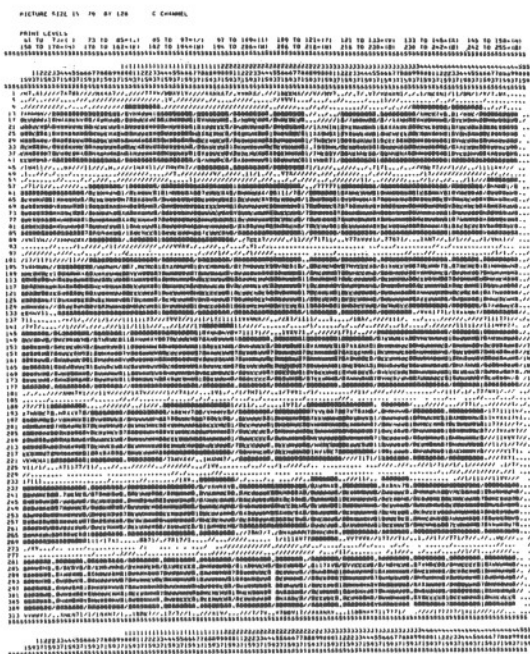


Figure 8 MB-2 Tree Boundaries

space can be calculated and then transformed back into the (W,I) space. In order to save processing, the second method is employed. A second pass is then made through the data to calculate the mean values of the data points whose coordinates are within the four color search regions. Pixels with coordinates outside of the four regions are not used in the calculations, since they are assumed to represent nontree information. The means are transformed into the (W,I) space and used as parameters in the decision functions which classify the trees in the next stage of processing. The transformed values are denoted by $U(LK,C)$ $LK = 1,2,3,4$, and $C = 1,2$; where LK represents the color: 1 = red, 2 = dark red, 3 = white, and 4 = black; and C specifies the coordinate: 1 = W and 2 = I.

The values of the variance parameters, $V(LK,C)$, $LK = 1,2,3,4$, and $C = 1,2$; are then calculated from the transformed widths of the four color search regions except for the following case. $V(3,2)$ is calculated using the distance between $U(3,2)$, the transformed intensity mean, and the transformed minimum intensity boundary for the white region, in order to limit the white response in the I direction. The variance parameter values are also used in the decision functions which subsequently classify the trees.

In the last stage of processing, the classification of each bounded object is determined. The classification is performed on an object by object basis, processing only pixels that lie within the rectangular boundaries. The values of two flags are required, one denoting the season of the year when the transparency was taken, the other denoting the presence or absence of heavy shadows.

The processing for each bounded area is as follows. First, $TNUM$, and the contents of arrays CLR , TPT , and CF , are set to zero. (The function of these variables will be described shortly.) Next, the state conditional probability density function¹⁷ is calculated for each of the pixels within the boundary:

$$P(\underline{PXL}(J,K)/LK) \approx \text{DEN}(LK) = \frac{1}{2} \exp\left(-\frac{(PXL(J,K,C) - U(LK,C))^2}{V(LK,C)}\right) \quad (8)$$

$C=1$

$LK=1,2,3,4$

where

$\underline{PXL}(J,K)$ is a vector composed of the (W,I) coordinate values at location (J,K).

LK denotes one of the four colors: red, dark red, white or black.

C denotes the coordinate.

$PXL(J,K,C)$ is an element of $\underline{PXL}(J,K)$, and

specifies a value of W or I at location (J,K).

U(LK,C) is the mean value for color class LK, in coordinate C.

V(LK,C) is the variance for color class LK, in coordinate C.

The form of DEN(LK) was chosen to be gaussian since the flying spot scanner was found to have a gaussian output when digitizing a slide containing a single color (i.e. a neutral density or Kodak wratten filter).

At each spatial location, the density function with the maximum value is determined:

$$\text{MAXCLS}(J,K) = \max(\text{DEN}(LK)) \quad (9)$$

LK

If MAXCLS(J,K) exceeds a threshold value of 0.1, the pixel is classified as color LK, the foliage color having the highest probability of causing PXL(J,K). MAXCLS(J,K) is then added to CLR(LK); and TPT(LK) and TNUM are incremented by one. Array CLR keeps a running total of the density values for each foliage color, TPT records the number of points receiving each color classification, and TNUM counts the total number of points within the boundary. If MAXCLS(J,K) does not exceed the threshold, no classification is made for that pixel, and no changes are made to CLR(LK), or to TPT(LK). TNUM, however, is incremented by one.

The threshold value was obtained by assuming that the distance from the mean was equal to the variance, and taking the resulting value, (0.362), as the threshold.

If pixels in two consecutive columns are both classified as color LK, the corresponding continuity function, CF(LK), is also incremented by one. (The last pixel in a row is consecutive with the first pixel in the next row.) CF keeps a running count of the relative size of continuous color areas that are contained within the boundary.

After all of the pixels within a given tree boundary have been processed, the color information is averaged over all of the points within the boundary:

$$\text{TCLR}(LK) = \text{CLR}(LK) / \text{TNUM} \approx P(\text{PXL}(J,K) / LK) P(LK) \quad (10)$$

LK = 1,2,3,4

where

$$P(\text{PXL}(J,K) / LK) \approx \text{CLR}(LK) / \text{TPT}(LK)$$

$$P(LK) \approx \text{TPT}(LK) / \text{TNUM}$$

Consequently, TCLR(LK) gives a relative measure of the amount of the characteristic color, LK, that is exhibited by the bounded object.

Before further processing is performed, the following ratio is calculated to verify that the bounded object exhibits tree-like color characteristics:

$$\text{TS} = \sum_{LK=1}^4 (\text{TPT}(LK)) \text{TNUM} \quad (11)$$

TS gives a total measure of the four characteristic foliage colors that are contained within the boundary. If TS is less than a threshold value, D2, the object is classified as a nontree, as shown in Table 2. This eliminates objects (i.e. patches of Johnson grass) that are similar in shape as the trees, but which exhibit different spectral characteristics. A nontree classification causes the classification to be stored, the following steps to be skipped, and processing to continue with the next boundary.

CONDITION	DECISION
TS < D2	NONTREE
DEC(3) > D3 AND DEC(3) > DECM·D4	GUMMOSIS
D5 ≤ DECM ≤ D6 AND DECM > DEC(3)·D7	MEALYBUG
DECM > D6 AND DECM > DEC(3)·D7	BROWN SOFT SCALE
OTHERWISE	HEALTHY

Table 2 Classification Decision Table

For the bounded objects that exhibit tree-like spectral characteristics, the following decision functions are calculated:

$$\text{DEC}(LK) = \text{TCLR}(LK) / \text{TCLR}(1), \quad LK = 2,3,4 \quad (12)$$

These functions are a modified form of the maximum likelihood ratio, and are formed from the ratio of the infested foliage colors to red, the healthy tree color.

A modified decision function, DECM, is calculated that combines the effect of the dark red and black foliage colors, and employs the continuity functions to assist in the separation of continuous dark color areas (brown soft scale), and areas that are mottled (mealybug):

$$\text{DECM} = \text{DEC}(2) + \text{DEC}(4) + 0.1(\text{CF}(2) + \text{CF}(4)) / \text{CF}(1) \quad (13)$$

Since shadows affect the value of DECM, a flag, SHAD, is set if the transparency contains heavy shadows. This causes DECM to be reduced by a factor of D1, so as to compensate for the extra dark information. Otherwise, the value of DECM is not affected. A second flag, SEAS, is also employed in order to prevent new foliage from being mistakenly identified as gummosis, since both have similar spectral characteristics during the spring and summer months. If SEAS is set, a classification of gummosis is prevented

in the following steps. Otherwise, the transparency was taken during the fall or winter months, and the classification is not affected.

DEC(3) and DECM are used to classify bounded (treelike) objects as shown in Table 2, using threshold values D3-D7. The derivation of the threshold levels is described in reference 14. Each object exhibiting treelike spectral characteristics is classified one of four ways: healthy, or containing gummosis, brown soft scale, or citrus mealybug. After each bounded object is classified, the result is stored, and after all of the bounded areas have been processed, the results are output in both tabular and pictorial (overprint) form.

IV RESULTS AND CONCLUSIONS

In order to test the recognition process, three of the training slides, MB-2, G-1, and BSS-19, were used to set the classification threshold levels, D2-D7, shown in Table 2. The system was then used to analyze six slides of unknown data. All of the slides contained only one type of infestation. The results were tabulated using the following index of recognition as a measure of recognition effectiveness:

$$I_q = N_q \times 100 / (N_q + M_q + L_q) \quad (14)$$

where

I_q is the index of recognition for the q th class of patterns, $0 \leq I_q \leq 100$ percent.

N_q is the number of patterns in class q that are correctly classified.

M_q is the number of patterns in class q that are misclassified into other classes.

L_q is the number of patterns in other classes that are misclassified into class q .

This index gives a measure of both commission and omission errors and is maximized if patterns in class q are not missed, and if patterns in other classes are not misclassified into class q . Note that non q classes of patterns are not individually specified in this expression.

The classification results for three typical slides are shown in Figures 9-11 in overprint form, and the results for all of the slides are tabulated in Tables 3-5. The classification key for the overprint output is shown in Table 6.

Tables 3-5 are tabulated by individual infestation, and also as infested/noninfested. In the latter case, no differentiation is made between the individual infestations in the infested category. I_q is calculated for the different classes shown in each table, using the corresponding values of N_q , M_q , and L_q . As an example,

for slide MB-2 in Table 3, MB denotes that class q represents trees infested with mealybug. Forty six trees containing mealybug were correctly classified, 6 were misclassified into other classes, and 3 healthy trees were misclassified as infested with mealybug, giving an index of recognition of 84%.

CLASS	N_q	M_q	L_q	$I_q (\%)$
<u>MB-2</u>				
MB	46	6	3	84
HEALTHY	35	3	5	81
ALL	81	9	8	83
INFESTED	47	5	3	85
NONINFESTED	35	3	5	81
ALL	82	8	8	84
<u>MR-13</u>				
MB	47	11	0	81
HEALTHY	0	0	4	0
ALL	47	11	4	76
INFESTED	51	7	0	88
NONINFESTED	0	0	4	0
ALL	51	7	4	82
<u>MB-20</u>				
MB	75	63	5	52
HEALTHY	83	20	17	69
ALL	158	83	22	60
INFESTED	120	18	5	84
NONINFESTED	83	20	17	69
ALL	203	38	22	77

Table 3 Index of Recognition of Mealybug

CLASS	N_q	M_q	L_q	$I_q (\%)$
<u>G-1</u>				
GUM	18	7	0	72
HEALTHY	50	1	4	91
ALL	68	8	4	85
INFESTED	18	7	0	72
NONINFESTED	50	1	4	91
ALL	68	8	4	85
<u>G-2</u>				
GUM	13	5	0	72
HEALTHY	39	13	2	72
ALL	52	18	2	72
INFESTED	13	5	13	42
NONINFESTED	39	13	2	72
ALL	52	18	15	61
<u>G-4</u>				
GUM	12	11	5	43
HEALTHY	18	21	10	37
ALL	30	32	15	39
INFESTED	13	10	21	30
NONINFESTED	18	20	10	38
ALL	30	30	31	33

Table 4 Index of Recognition of Gummosis

Slide G-4 received the lowest recognition rate. It contained very heavy shadows, and several of the trees were surrounded with Johnson grass, an indication that the grove was not well taken care of. The shadow information caused many of the healthy trees to be classified as infested with mealybug, while many of the trees infested with gummosis were classified as healthy, since the ratio of white to dark information was shifted to below the gummosis threshold. Also, several of the trees surrounded with Johnson grass

received the classification of gummosis, because of the extra white information introduced by the grass. For this slide, the index of recognition for healthy trees was 37%, while the value for infested trees was 43%.

CLASS	N _q	M _q	L _q	I (X) q
BSS-19				
BSS	15	2	0	88
HEALTHY	1	0	0	100
ALL	16	2	0	89
INFESTED	16	1	0	94
NONINFESTED	1	0	0	100
ALL	17	1	0	94
BSS-18				
BSS	14	15	1	47
HEALTHY	7	0	2	78
ALL	21	15	3	54
INFESTED	26	3	1	87
NONINFESTED	7	0	2	78
ALL	33	3	3	85
BSS-20				
BSS	52	15	5	72
HEALTHY	0	1	0	0
ALL	52	16	5	71
INFESTED	52	15	5	72
NONINFESTED	0	1	0	0
ALL	52	16	5	71

Table 5 Index of Recognition of Brown Soft Scale

GRAPHICAL REPRESENTATION	CLASSIFICATION
BLACK BORDER	HEALTHY
GRAY RECTANGLE	MEALYBUG
BLACK RECTANGLE	BROWN SOFT SCALE
WHITE RECTANGLE	GUMMOSIS
WHITE BORDER	NONTREE

Table 6 Classification Key

Another problem was the cross classification of citrus mealybug with brown soft scale. Slide BSS-18 contained infestations of brown scale that ranged from very light to very heavy. Many of the lightly infested trees had the appearance of being infested with citrus mealybug, and were misclassified into that category. In contrast, slide MB-20 contained infestations of mealybug with very heavy concentrations of sooty mold, and many of the infested trees were misclassified as containing brown soft scale. When the results were reclassified using the infested/noninfested classes, the index of recognition changed from 47 to 87%, and from 52 to 84%, respectively, for the two slides.

Unknown slides MB-13, G-2, and BSS-20 returned values of I_q for the three infestation classes that were higher than in the previous examples. The images contained only light to moderate shadows, and were taken of citrus groves that were well maintained; slides BSS-20 and MB-13 contained infestations of brown soft scale and citrus mealybug that exhibited distinctive visual characteristics. The index of recognition values for these slides ranged from 72 to 81% for the three infestations.

(The value for healthy trees was zero for MB-13 which contained no healthy trees, and for BSS-20 which contained only one healthy tree.) These results used in conjunction with the previous values, show that the system achieves nominal recognition values of 60 to 80% for each of three infestations.

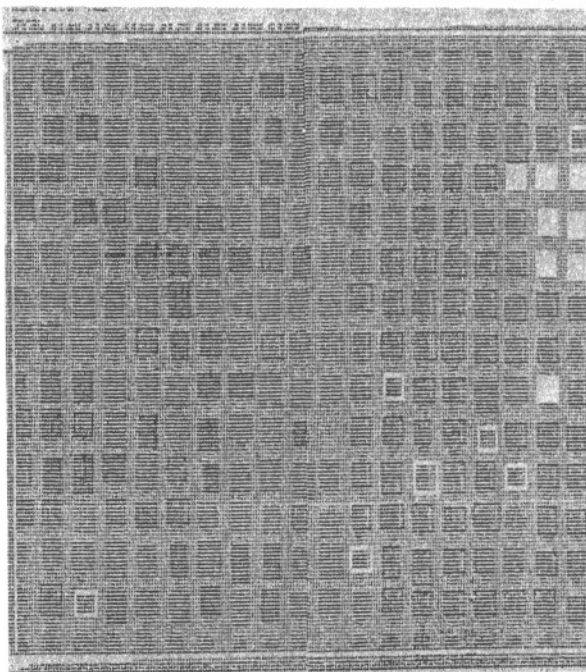


Figure 9 MB-20 Tree Classification

In conclusion, the system detects the presence of citrus mealybug, brown soft scale, and Rio Grande gummosis in individual citrus trees using only four parameters as input. Moderate shadows had no undue effect upon the classification process, but heavy shadows caused a significant increase in the classification error rate. Moderate infestations of mealybug were separated from moderate to heavy infestations of brown soft scale, however, heavy infestations of mealybug, and light infestations of brown soft scale were not effectively separated by the system. The spectral information is the primary feature that is used to recognize the infestations. Although three times as much data must be initially processed in comparison to black and white values, typically, less than 1.5 times as much data is required for the majority of processing.

The transparencies were provided by USDA ARS, 509 W. 4th Street, Weslaco, Texas, with special assistance given by M. R. Davis, and S. J. Ingle.

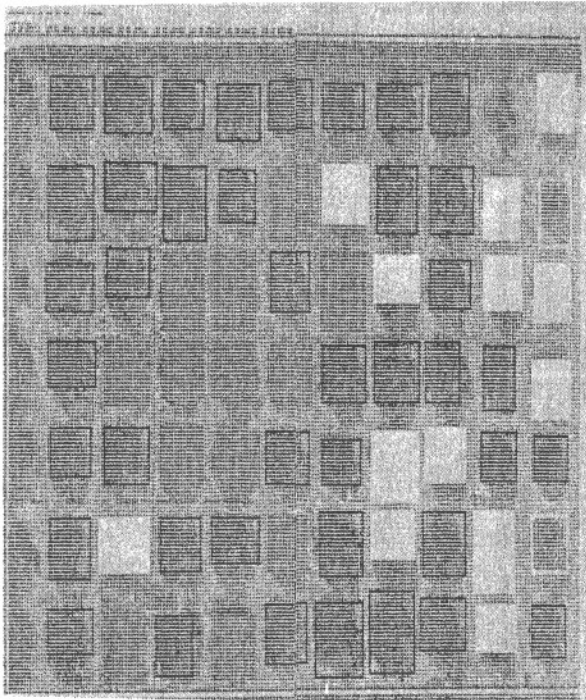


Figure 10 G-2 Tree Classification

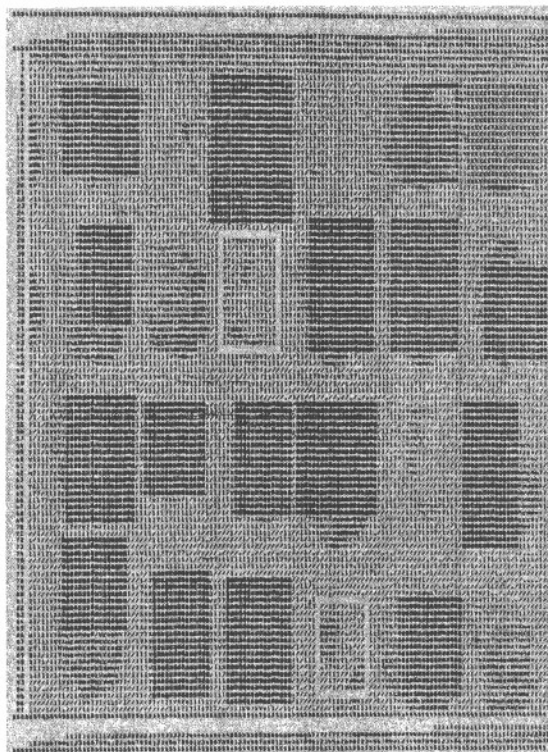


Figure 11 BSS-19 Tree Classification

1. Hart, W. G., S. J. Ingle, M. R. Davis, C. Mangum, A. Higgins, and J. C. Boling, "Some Uses of Infrared Aerial Color Photography in Entomology," Proceedings of the Third Biennial Workshop on Color Aerial Photography in the Plant Sciences, Gainesville, Florida, pp 99-113, March 2-4, 1971.
2. Hart, W. G. and S. J. Ingle, "Detection of Arthropod Activity on Citrus Foliage with Aerial Infrared Color Photography," Proceedings, Workshop on Aerial Color Photography in the Plant Sciences, Gainesville, Florida, pp 85-88, March 5-7, 1969.
3. Hart, W. G. and V. I. Meyers, "Infrared Aerial Color Photography for Detection of Populations of Brown Soft Scale in Citrus Groves," Journal of Economic Entomology, Vol. 61, pp 617-624, June 1968.
4. Edwards, George J., Tom Schehl and E. P. DuCharme, "Multispectral Sensing of Citrus Young Tree Decline," Photogrammetric Engineering and Remote Sensing, Vol. 41, pp 653-657, May 1975.
5. Hart, W. G., S. J. Ingle, M. R. Davis, and C. Mangum, "Aerial Photography with Infrared Color Film as a Method of Surveying for Citrus Blackfly," Journal of Economic Entomology, Vol. 66, pp 190-194, February 1973.
6. Davis, M. R., "Photointerpreter Key," Private Communication to J. K. Aggarwal, S. A. Underwood, and D. H. Williams, 1974.
7. Norman, Gerald G. and Norman L. Fritz, "Infrared Photography as an Indicator of Disease and Decline in Citrus Trees," Proceedings, Florida State Horticultural Society, Vol. 78, pp 59-63, 1965.
8. Underwood, S. A. and J. K. Aggarwal, "Interactive Computer Analysis of Aerial Color Infrared Photographs," Computer Graphics and Image Processing, Vol. 6, No. 1, pp 1-24, February 1977.
9. Ali, M. and J. K. Aggarwal, "Automatic Detection and Classification of Infestations of Crop Insect Pests and Diseases from Infrared Aerial Color Photographs," Proceedings, Symposium on Machine Processing of Remotely Sensed Data, Purdue University, West Lafayette, Indiana, June 29-July 1, 1976.
10. Pratt, Robert M., "Florida Guide to Citrus Insects, Diseases and Nutritional Disorders," Agriculture Experiment Station, Gainesville, Florida, April 1958.
11. Knipling, Edward B., "Physical and Physiological Basis for the Reflectance of Visible and Near Infrared Radiation from Vegetation," Remote Sensing of Environment, Vol. 1, pp 155-159, Summer 1970.

12. Underwood, S. A., D. H. Williams, P. Costa and J. K. Aggarwal, "A Flying Spot Scanner System," ISA Transactions, Vol. 14, No. 4, pp 340-357, 1975.
13. Yachida, Masahiko, and Saburo Tsuji, "Application of Color Information to Visual perception," Pattern Recognition, Vol. 3, pp 307-323, 1971.
14. Williams, D. H., "Computer Detection of Citrus Infestations Using Aerial Color Infrared Transparencies," Ph. D. dissertation, The University of Texas at Austin, May 1977.
15. Williams, D. H. and J. K. Aggarwal, "Computer Location of Citrus Trees Using Color Aerial Infrared Transparencies," Proceedings, Symposium on Machine Processing of Remotely Sensed Data, Purdue University, West Lafayette, Indiana, June 29-July 1, 1976.
16. Davis, Larry S., "A Survey of Edge Detection Techniques," Computer Graphics and Image Processing, Vol. 4, No. 3, pp 248-270, September 1975.
17. Duda, Richard O. and Peter E. Hart, "Pattern Classification and Scene Analysis," Wiley-Interscience, New York, New York, 1973.

David H. Williams received the BSEE degree from New Mexico State University in 1968, an MS from the University of New Mexico in 1971, and the Ph.D from the University of Texas at Austin in 1977, all in Electrical Engineering. From 1968 to 1970 he worked as a Reactor Safety Engineer for the U. S. Atomic Energy Commission in Albuquerque N.M., and from 1976 to 1978 he was a Visiting Assistant Professor in the EECS department at the University of New Mexico. Since September, 1978 he has been an Assistant Professor of Electrical Engineering at The University of Texas at El Paso.

J. K. Aggarwal received his BS in mathematics and physics from the University of Bombay (1956), B. Eng from the University of Liverpool, England (1960), and MS and Ph.D from the University of Illinois in 1961 and 1964, respectively. Since 1964, he has been at the University of Texas at Austin where he is currently a Professor of Electrical Engineering and of Computer Science. Dr. Aggarwal has published numerous technical papers, and several books, and he is an active member of the IEEE, Pattern Recognition Society, and Eta Kappa Nu. His current research interests are digital filters, computational methods, and image processing.